Revealing how variations in antibody repertoires correlate with vaccine responses

Yana Safonova[1,2], Sung Bong Shin[3], Luke Kramer[4], James Reecy[4], Corey T. Watson[2], Timothy P.L. Smith[3], and Pavel A. Pevzner[1,*]

[1] Computer Science and Engineering Department, University of California San Diego, San Diego, CA, USA

[2] Department of Biochemistry and Molecular Genetics, University of Louisville School of Medicine, Louisville, KY, USA

[3] U.S. Meat Animal Research Center, USDA-ARS, Clay Center, NE, USA

[4] Department of Animal Science, Iowa State University, Ames, IA, USA

[*] Corresponding author: ppevzner@eng.ucsd.edu

Abstract

An important challenge in vaccine development is to figure out why a vaccine succeeds in some individuals and fails in others. Although antibody repertoires hold a key to answering this question, there have been very few personalized immunogenomics studies so far aimed at revealing how variations in immunoglobulin genes affect a vaccine response. We conducted an immunosequencing study of 204 calves vaccinated against bovine respiratory disease (BRD) with the goal to reveal variations in immunoglobulin genes and somatic hypermutations that impact the efficacy of vaccine response. Our study represents the largest longitudinal personalized immunogenomics study reported to date across all species, including humans. To analyze the generated dataset, we developed an algorithm for identifying variations of the immunoglobulin genes (as well as frequent somatic hypermutations) that affect various features of the antibody repertoire and titers of neutralizing antibodies. In contrast to relatively short human antibodies, cattle have a large fraction of ultralong antibodies that have opened new therapeutic opportunities. Our study revealed that ultralong antibodies are a key component of the immune response against the costliest

disease of beef cattle in North America. The detected variants of the cattle immunoglobulin genes, which are implicated in the success/failure of the BRD vaccine, have the potential to direct the selection of individual cattle for ongoing breeding programs.

Introduction

The challenge of identifying variations in immunoglobulin genes that affect vaccine response. Although vaccination is a primary tool to control the spread of viral and bacterial diseases, the success of vaccines at the population level does not always translate to protection at the individual level. Figuring out why a vaccine fails in some individuals is important both during the vaccine development stage (to inform changes in the vaccination protocols) and the vaccine administration stage (to identify a sub-population with a poor vaccine response). A promising approach to understanding why a vaccine succeeds in some individuals and fails in others is to analyze the germline variations in the immunoglobulin (IG) loci of individuals with successful/failing antibody responses to the vaccine.

Antibodies are not encoded in the germline genome but rather result from somatic genomic recombinations called *VDJ recombinations* (Tonegawa, 1983). This process affects an IG locus containing the families of the *variable* (*V*), *diversity* (*D*), and *joining* (*J*) genes (referred to as *IG genes*) by selecting one V, one D gene, and one J gene, and concatenating them together to generate one of the antibody chains. Further diversity of antibodies is generated by the class-switch recombination and somatic hypermutations (SHMs) (Dudley et al. 2005). There are three types of IG loci in mammalian species (including cows): heavy chain, kappa light chain, or lambda light chain. In this work, we focus on the heavy chain (IGH) locus only.

The *expression quantitative trait loci* (*eQTL*) analysis links variation in gene expression to genotypes. Although eQTL analysis has greatly contributed to the dissection of the genetic basis of disease and vaccine response (Franco et al., 2013, Bhalala et al., 2018), the IG loci remain virtually untouched by eQTL studies

(Watson et al., 2017). eQTL studies usually start from generating an *n*×*m genotype matrix* that contains information about each of *m* markers (e.g., SNPs) in each of *n* individuals and an *n*×*k phenotype (expression) matrix* that contains information about expression levels of each of *k* genes in each of *n* individuals. Generating analogs of the genotype and phenotype matrices in immunogenomics studies is a more complex task than in traditional eQTL studies.

First, while the set of genes in eQTL studies is fixed and shared by all individuals, the antibody repertoire is composed of a virtually unlimited set of proteins, and there are typically few antibodies shared between any two individuals. Thus, given an antibody repertoire represented as a *repertoire sequencing* (*Rep-seq*) dataset, it is not clear how to define the phenotype matrix. One possibility is to consider each germline gene in the IG locus (e.g., a V gene, a D gene, or a J gene) and to define the *usage* of this gene as the fraction of antibodies that originated from this gene among all antibodies in the Rep-Seq dataset. Our goal is to identify *usage QTLs* (*IgQTLs*) that link variation in usage to a genotype.

Second, eQTL studies are usually based on RNA-seq and Whole Genome Sequencing (WGS) data, while immunosequencing studies generate Rep-seq data about antibodies. Thus, the genotype matrix in immunosequencing studies has to be inferred from Rep-seq data alone since the WGS data is typically not available. Although inference of alleles of V, D, and J genes from Rep-seq data is a well-studied problem (Gadala-Maria et al., 2015; Corcoran et al., 2016; Gadala-Maria et al., 2019; Safonova and Pevzner, 2019; Bhardwaj et al., 2020), the existing allele inference tools, primarily developed for naïve repertoires, often fail in the case of more complex antigen-stimulated repertoires that represent the primary goal of IgQTL studies. Also, in contrast to allele inference tools that attempt to infer SNPs and ignore frequent somatic hypermutations, IgQTL studies should account for both SNPs and frequent SHMs since they may play equally important roles in vaccine responses.

Bovine Respiratory Disease. We conducted a personalized immunogenomics study of 204 calves to analyze the efficacy of the bovine respiratory disease (BRD) vaccine, the largest time-series immunosequencing dataset generated so far across all species, including human. Since cattle production accounted for $67 billion in 2018 in the United States (Economic Research Service USDA, 2021), maintaining cattle health is an important direction of agricultural studies. The BRD is the costliest disease of beef cattle in North America (Taylor et al., 2010). Although vaccination reduces the risk of BRD, losses from BRD remain substantial and individuals respond very differently to the BRD vaccine (Kramer et al., 2017). In order to understand links between variants in cattle IG genes and antibody responses to the vaccine, we generated four Rep-Seq datasets (taken before and after the BRD vaccination) for each of 204 calves.

Ultralong cattle antibodies. The evolution of the cattle IGH locus has resulted in a loss of many functional V genes, thus reducing the diversity of the cattle antibody repertoire (Haakenson et al., 2018). To compensate for the reduced VDJ recombination diversity, cattle have developed antibodies with ultralong CDR3s that have a unique mechanism of *structural diversification* (Dong et al., 2019). We refer to antibodies with CDR3s longer than 50 amino acids as *ultralong antibodies* (for comparison, the average length of human CDR3s is only 15 aa). Although non-conventional recombination processes (such as D-D fusions and V gene replacement) can generate ultralong human antibodies (including, broadly neutralizing human antibodies against HIV-1, Yu and Guan, 2014), they are rare in human antibody repertoires, typically accounting for less than 1% of all antibodies (Safonova and Pevzner, 2019). In contrast, ultralong antibodies account for ~10% of cattle antibodies (Wang et al., 2013).

The vast majority of ultralong cattle antibodies are generated by the VDJ recombination of the same V, D, and J genes: IGHV1-7, IGHD8-2, and IGHJ2-4 (Wang et al., 2013). An unusually long IGHD8-2 gene (148 nt) contributes to all ultralong CDR3s and enables their structural diversification. This gene encodes four

cysteines that form disulfide bonds and turn the CDR3 loop into a complex protein structure called a *knob* (Wang et al., 2013). IGHD8-2 also contains many codons that differ from the cysteine codons by a single nucleotide. SHMs often result in new cysteines that form new disulfide bonds, thus extending the diversity of the knob structures.

Ultralong cattle antibodies open new therapeutic opportunities (Muyldermans and Smider, 2016) and may even neutralize various strains of HIV (Sok et al., 2017). Human antibodies target the HIV envelope glycoprotein (*Env*) presented on the virus surface. However, highly mutated *Env* proteins are often covered by glycans, making them a hard-to-reach target for human antibodies. Ultralong cattle antibodies penetrate glycans and directly target the conservative sites that are unreachable for human antibodies since they are buried inside the *Env* protein. Although ultralong cattle antibodies have great pharmaceutical potential in terms of targeting unusual antigens (Burke et al., 2020), their role in the native immune response remains unclear.

The challenge of finding IgQTLs. Previous immunosequencing studies have succeeded in linking variants in the human IGH locus to disease and vaccination efficacy (Thomson et al., 2008; Lingwood et al, 2012; Avnir et al., 2016; Parks et al., 2017, Lee et al., 2021, Mikocziova et al., 2021) but have not yet resulted in a software tool addressing the above-mentioned complications in finding IgQTLs. We thus developed the IgQTL tool for detecting both variants of germline V genes and their frequent SHMs for downstream analysis of usage QTLs in the V genes. Using IgQTL, we inferred genotypes associated with the fraction of ultralong antibodies in a repertoire, and the fraction of antibodies specific to BRD antigens. Our findings indicate that ultralong antibodies play an important role in the bovine antibody response against BRD antigens and suggest that it is important to add immunosequencing to the existing genomics-based breeding efforts in the cattle industry.

Results

Rep-Seq datasets. We analyzed Rep-seq datasets for 204 purebred American Angus calves vaccinated against BRD. Each animal was initially vaccinated at day 0 and then given a booster vaccination three weeks later (Figure 1A). For each animal, four IgG samples were collected: three weeks prior to vaccination (referred to as "–3"), at the moment right after the first vaccination (referred to as "0"), three weeks post-vaccination (referred to as "+3"), and six weeks post-vaccination (referred to as "+6"). Serum from each of the sequenced animals was also assayed for BRD-specific antibody titers at the same time points (Kramer et al., 2017) to quantify pre-existing immunity (e.g., resulting from maternal antibodies that are passed through milk from the mother to the child) and as a measure of vaccine success.

High-usage cattle V genes. Each Rep-Seq dataset was aligned to 13 cattle V genes from IMGT, the international ImMunoGeneTics information system (Lefranc et al., 2009) (see Methods). For each V gene, we computed its usage in an individual as the fraction of sequences with distinct CDR3s aligned to this V gene in the corresponding Rep-Seq dataset. We defined the *average usage* of a V gene as its average usage across all individuals and all time points. Only 8 out of 13 V genes had an average usage exceeding 0.01: IGHV1-7, IGHV1-10, IGHV1-14, IGHV1-17, IGHV1-20, IGHV1-21, IGHV1-27, and IGHV1-30. We refer to them as *high-usage* V genes and limit further analysis to these genes only.

IGHV1-7 is the only V gene with a statistically significant increase in usage after vaccination. We first assessed differences in usage between pre- and post-vaccination for all V genes. We found that only IGHV1-7 has significantly higher usage after the vaccination (Table S1). Figure 1B shows that the usage of the IGHV1-7 gene is significantly increased at time points "+3" and "+6" (P-value=8.17×10^{-115}), suggesting that vaccination triggered the production of antibodies derived from IGHV1-7. Henceforth, we

used the linear mixed effect model to estimate P-values (referred to simply as "P") for repeated measures (representing four time points), unless a different method is specified.

Analysis of Rep-seq datasets collected at the time point "–3" revealed that each V gene but IGHV1-7 has positive or negative correlation of usages with other IGHV genes. Figure 1C shows that V genes form three groups based on their usage, consisting of seven positively correlated genes: G1=(IGHV1-10, IGHV1-14), G2=(IGHV1-17, IGHV1-20, IGHV1-30), and G3=(IGHV1-21, IGHV1-27). IGHV1-7 is the only gene with an independent usage profile. These correlations are consistent across time points "0", "+3", and "+6". We conjecture that this is explained by an association of IGHV1-7 with ultralong CDR3s and their special role in the adaptive immune response. Figure 1C illustrates that the usages in groups G1, G2, and G3 anticorrelate.

BRD vaccination triggers the increased production of ultralong antibodies. Figure 1D shows that for all high-usage cattle V genes, except for IGHV1-7, the mean CDR3 length does not exceed 75 nt. It also illustrates that, unlike other V genes, IGHV1-7 has a bimodal distribution of CDR3 lengths, and the second mode is represented by ultralong CDR3s. On average, 21% of sequences derived from IGHV1-7 have ultralong CDR3s at time point "–3" and 99% of ultralong CDR3s across all individuals are derived from IGHV1-7. The latter observation agrees with findings reported by Walther et al., 2013, Wang et al., 2013, Deiss et al., 2017, and Dong et al., 2019.

Figure 1E illustrates that both initial and booster vaccinations significantly increase the fraction of ultralong CDR3s in all CDR3s (across all V genes) at time points "+3" and "+6" ($P=3.61\times10^{-107}$). Figure 1F shows that the fraction of ultralong CDR3s in all CDR3s derived from IGHV1-7 also increases after vaccinations ($P=1.19\times10^{-119}$). These observations suggest that the vaccination triggers the production of antibodies derived from IGHV1-7.

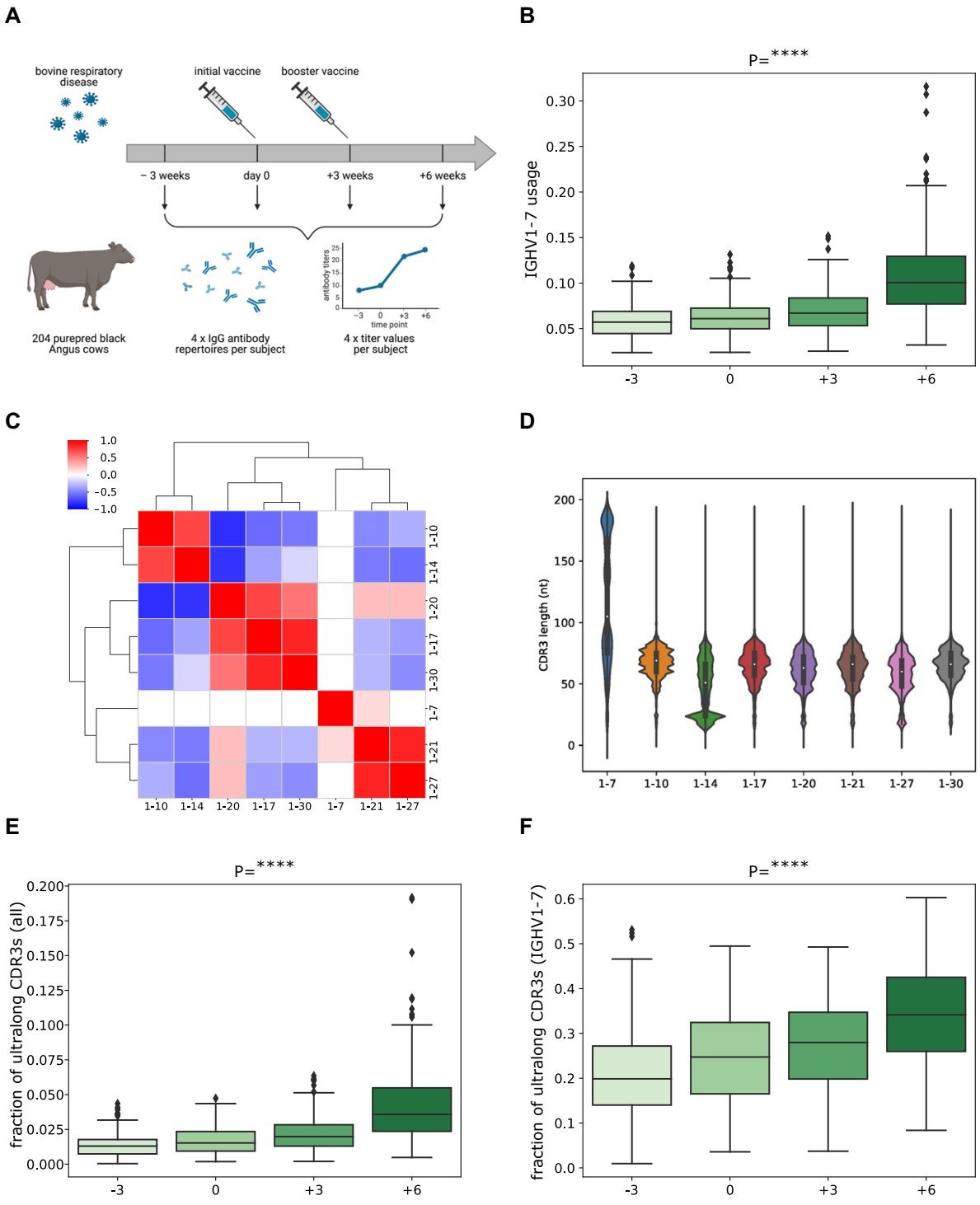

170 **Figure 1. Overview of study design and characteristics of antibody repertoires.** (*A*) The panel shows an overview
171 of the study design. 204 calves were vaccinated against BRD, and their expressed antibody repertoires were sequenced
172 at four time points pre- and post-vaccination. Serum from each of the sequenced animals was also assayed for BRD-

specific antibody titers at the same time points. (*B*) The distribution of IGHV1-7 usage at four time points. Here and further, each box shows the quartiles of the distribution. The whiskers show the rest of the distribution, except for outliers found using a function of the inter-quartile range implemented by the Seaborn package in Python. P-values have the following notation: ns≥0.05, *<0.05, **<0.01, ***<0.001, ****<0.0001. (*C*) The matrix shows the Pearson correlations between gene usages computed across all high-usage V genes at time point "–3". Correlation values vary from –1 (blue) to 1 (red). Statistically insignificant correlations (P≥0.05) are shown as white cells. (*D*) The histogram of the distributions of the CDR3 lengths for eight highly-used cattle V genes. The histogram is computed for individual 14007. (*E*) The distribution of the fraction of ultralong CDR3s in all CDR3s at four time points. (*F*) The distribution of the fraction of ultralong CDR3s in CDR3s derived from IGHV1-7 at four time points.

Antibody titers correlate with fractions of ultralong CDR3s. Some calves have pre-existing immunity because they either were previously exposed to the BRD-causing virus or have maternal antibodies specific to BRD. This pre-existing immunity (as well as cross-reactivity of antibodies) may affect titers at the initial time point "–3". Downey et al., 2013 demonstrated that the decay rate of maternal antibodies is rather low and that there is a threshold effect: the calves do not respond to the vaccine if the level of maternal antibodies exceeds a threshold and only respond when this level drops. Also, the impact of calf age on antibody response (titers) to BRD was previously shown to be insignificant (Kramer et al., 2017).

Figure 2A shows that, on average, the booster vaccination increased neutralizing antibody titers. Figure 2B shows the Pearson correlation r between antibody titers at four time points and illustrates that they correlate at points "–3" and "0" (r=0.78, P=5.83×10^{-43}), "–3" and "+3" (r=0.43, P=1.53×10^{-10}), and "0" and "+3" (r=0.43, P=2.29×10^{-10}). In contrast, antibody titers from time points "–3" and "0" anticorrelate with final titers at the time point "+6" (r=–0.42, P=3.34×10^{-10} and r=–0.4, P=1.78×10^{-9}, respectively). This suggests that pre-existing immunity to BRD antigens may be suboptimal, preventing development of a successful immune response to the BRD vaccine. Impacts of suboptimal antibody responses caused by pre-existing immunity were reviewed by Zimmermann and Curtis, 2019 (for various antigens) and Iwasaki and Yang,

198 2020 (for SARS-CoV-2) and discussed in Supplemental Note "The relations between pre- and post-
199 vaccination immunity to the BRD vaccine in calves".

200

201 We have not found any statistically significant correlations between the titers and the usages of all high-
202 usage V genes, except for IGHV1-7. Both the usage of IGHV1-7 (Figure 2C) and the fraction of ultralong
203 CDR3s (Figure 2D) at the time point "+3" correlate (albeit weakly) with final titers at the time point "+6"
204 (r=0.25, P=0.0004, and r=0.18, P=0.0125, respectively). These observations support our hypothesis that
205 antibodies with ultralong CDR3s play an important role in recognizing the vaccine antigens.

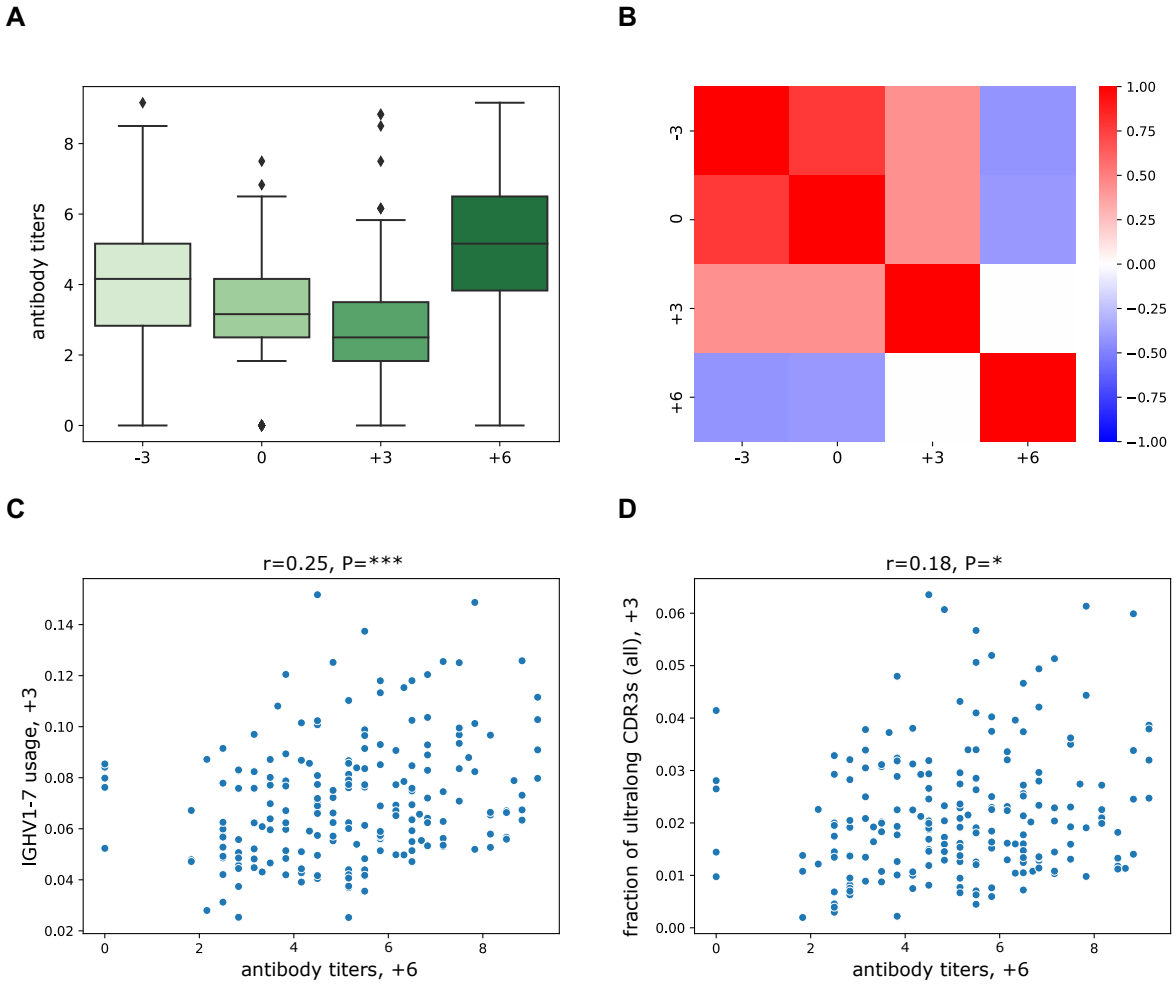

206 **Figure 2. Antibody titers statistics.** (*A*) The distribution of antibody titers at four time points. Titers at time point
207 "-3" show the number of BRD-specific antibodies without any antigen stimulation. Titers at time point "0" represent

208 immediate memory responses triggered by the vaccine. Titers at time points "+3" and "+6" reflect antibodies produced
209 as a result of the vaccination. Details of the titer analysis are described in Kramer et al., 2017. (*B*) The matrix shows
210 the Pearson correlations between antibody titers at four time points. Correlation values vary from –1 (blue) to +1 (red).
211 Statistically insignificant correlations (P≥0.05) are shown as white cells. (*C*) Antibody titers at time point "+6" vs
212 usages of IGHV1-7 at time point "+3". (*D*) Antibody titers at time point "+6" vs fractions of ultralong CDR3s in all
213 CDR3s at time point "+3". The Pearson correlations (*r*) and P-values (P) are shown at the top of panels (*C*) and (*D*).

214 **The IgQTL pipeline.** To reveal the associations between germline/somatic variants and features of cattle
215 antibody repertoires (gene usages, antibody titers, and fractions of ultralong antibodies), we developed the
216 IgQTL tool. IgQTL takes Rep-Seq reads and antibody titers (if available) as an input and consists of the
217 following steps (Figure 3A):

218 • Generating the phenotype matrix containing information about gene usages, fractions of ultralong
219 CDR3s, antibody titers, etc.
220 • Finding germline and somatic variations (GSVs).
221 • Generating and clustering a genotype matrix to reveal subjects with common genotypes.
222 • Finding statistically significant genotype-phenotype associations.
223 • Identifying the most consequential GSVs with respect to phenotypes.

224 Below we applied IgQTL to reveal the genotype-phenotype associations in the cattle immunosequencing
225 study.
226
227 **Generating the phenotype matrix.** The phenotype matrix is defined as a matrix with 204 rows, where
228 each column represents either the usage of one of V genes, or the fraction of ultralong antibodies, or an
229 antibody titer. In the case of the cattle immunosequencing dataset, IgQTL forms a 204×14 phenotype matrix
230 that represents usages of all high-usage V genes (the first eight columns), the fraction of ultralong antibodies
231 among all antibodies in the repertoire (9^{th} column), the fraction of ultralong antibodies derived from

IGHV1-7 among all antibodies derived from IGHV1-7 (10^{th} column), and the antibody titers (the last four columns).

Finding germline variations and frequent SHMs in the V genes. Previous studies have revealed associations between germline variations in V genes and variation in their usages and antibody titers (Thomson et al., 2008; Lingwood et al, 2012; Avnir et al., 2016; Parks et al., 2017, Lee et al., 2021, Mikocziova et al., 2021). However, these studies did not consider the impact of frequent SHMs that, similarly to germline variations, may be associated with variation in gene usage. Since the Rep-Seq data, obtained from IgG antibodies, represent mature antibody responses, below we analyzed the impact of frequent SHMs on antibody repertoires.

To capture both germline variations and frequent somatic hypermutations (further referred to as *germline or somatic variations* or *GSVs*) for each subject, we generated a *combined* dataset from all four time points by collapsing identical sequences and analyzed sequences aligned to the same V gene. Given a position in a germline V gene, we analyzed all reads aligning to this gene in a single combined dataset and computed a vector (f_A, f_C, f_G, f_T), where f_N is the fraction of reads that have the nucleotide N aligned at this position. We collected such vectors from all subjects and define $N1$ and $N2$ as nucleotides with the highest and the second-highest total fractions.

For most positions, f_{N1} is close to 1, indicating that these positions do not exhibit variations and frequent SHMs. We were interested in positions where f_{N1} falls below a *frequency threshold freq* (the default value *freq*=0.55) as such positions likely reflect one of the following situations:

- if a subject is homozygous by $N2$ (i.e., $N1$ is substituted by $N2$ in the germline), we expect that f_{N1}~0 and f_{N2}~1.
- if a subject is heterozygous by $N1/N2$, we expect that f_{N1}~0.5 and f_{N2}~0.5.

- if the germline nucleotide $N1$ is replaced by a frequent SHM represented by $N2$ (with frequency at least 50%), we expect that $f_{N1} \leq freq$.

We classified a position P in a gene G as a GSV if $f_{N1} \leq freq$ for at least one subject.

Each *GSV* (represented by a position P in a gene G, and nucleotides $N1$ and $N2$) was encoded as (P, G, $N1/N2$). Figure 3B illustrates the procedure for identifying GSVs using examples of a GSV (126, IGHV1-7, A/G) that represented a known germline variation, a GSV (167, IGHV1-10, G/A) that represents a likely frequent SHM, as well as a non-GSV (180, IGHV1-27, C/T).

Fractions f_{N1} for position 126 in IGHV1-7 vary from 0.01 to 0.98 and form a trimodal distribution. Since GSV (126, IGHV1-7, A/G) is a known germline variant, the three modes correspond to the homozygous states AA and GG, and a heterozygous state AG. (126, IGHV1-7, A/G) is classified as a GSV because the minimum of fractions f_{N1} across all individuals (0.01) does not exceed the default frequency threshold $freq$=0.55. (167, IGHV1-10, G/A) was classified as a GSV because fractions f_{N1} for position 167 of IGHV1-10 vary from 0.54 to 0.86 (likely frequent SHM). In contrast, (180, IGHV1-27, C/T) was classified as non-GSV since fractions f_{N1} for position 180 in IGHV1-27 vary from 0.78 to 0.95 and did not fall below the frequency threshold.

In total, we classified 52 GSVs in seven V genes: IGHV1-7 (8 GSVs), IGHV1-10 (10), IGHV1-14 (3), IGHV1-17 (7), IGHV1-20 (8), IGHV1-21 (8), and IGHV1-27 (8). 17 out of 52 GSVs represent known germline variations (Figure S1).

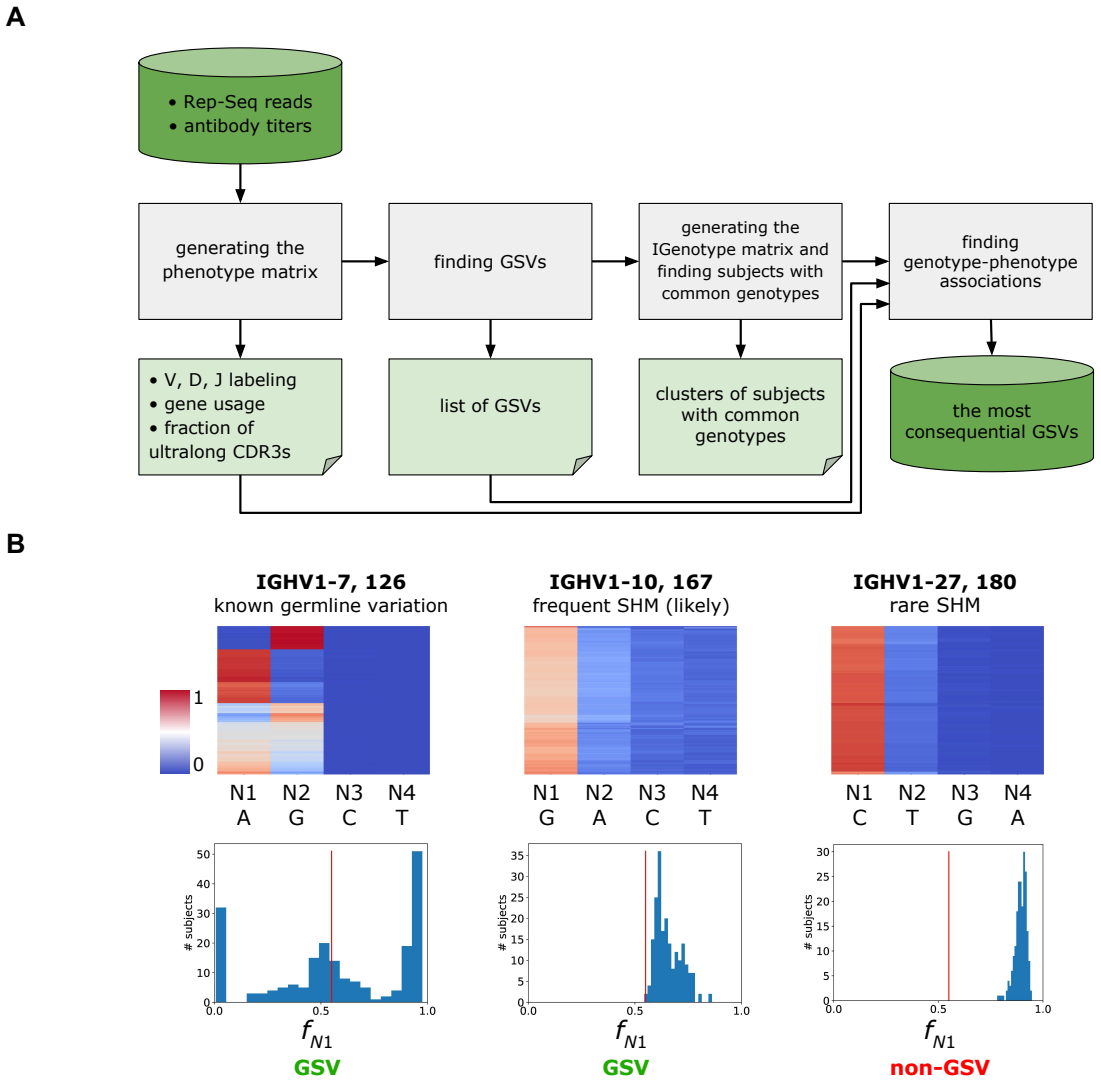

278 **Figure 3. Overview of IgQTL method.** (*A*) The panel illustrates IgQTL pipeline. Grey rectangles show various steps
279 of the IgQTL pipeline. The input (Rep-Seq reads and antibody titers) and the final output (the most consequential
280 GSVs) are shown in bright green. Intermediate output is shown in light green. (*B*) The panel illustrates the procedure
281 for finding GSVs (126, IGHV1-7, A/G) and (167, IGHV1-10, G/A), as well as non-GSV (180, IGHV1-27, C/T).
282 Heatmaps in the upper row show the fractions of the nucleotides across all subjects varying from 0 (blue) to 1 (red).
283 Columns are arranged according to the sum of fractions across all subjects. *N*1 and *N*2 correspond to the first and the
284 second columns, respectively. Histograms in the lower row show distributions of fractions f_{N1} across 204 animals. The
285 red vertical line in each histogram corresponds to *freq*=0.55.

Generating the genotype matrix. For each GSV (*P*, *G*, *N*1/*N*2) in each animal, IgQTL computes the *R*-*ratio* as $R = f_{N1} / (f_{N1} + f_{N2})$. The *R*-ratio represents a more flexible and expressive alternative to the conventional binary description of SNP states (e.g., A/A or A/C) because it enables description of SHMs and their relative abundance. The *R*-ratios also distinguish subjects that are heterozygous by the same pair of alleles but have different expression profiles for these alleles (e.g., 80%-20% vs 50%-50%).

We refer to a 52-mer vector of all *R*-ratios for a given animal (across all GSVs) as its *IGenotype*. We further analyzed IGenotypes across all 204 animals for finding their correlations with various phenotypes. The IGenotypes of 204 animals across 52 GSVs form a 52×204 *IGenotype matrix*, an analog of a genotype matrix that describes both genomic SNPs and SHMs (Figure 4A).

Clustering animals with similar IGenotypes. We clustered animals into groups with similar IGenotypes (these groups represent analogs of common genotypes) by applying the principal component analysis (PCA) to the IGenotype matrix. Iterative *k*-means clustering of the first two principal components with *k* from 2 to 10 followed by the elbow method (Thorndike, 1953) reveals that k=3 provides the optimal decomposition of 204 animals (Figure 4B, Figure S2). Although decompositions into more clusters resulted in similar values of inertia (Figure S2), we focused our analysis on k=3 because it simplified further statistical analysis and allowed us to apply popular statistical methods such as the Kruskal-Wallis test (Kruskal and Wallis, 1952).

We say that the computed clusters are *associated* with the *R*-ratios (or usages/titers/fractions of ultralong CDR3s) if the differences between distributions of *R*-ratios (or usages/titers/fractions of ultralong CDR3s) across these clusters are statistically significant. The computed clusters C1, C2, and C3 are associated with the *R*-ratios for 47 out of 52 GSVs, including 16 out of 17 known germline variations (Figure S3). We thus

conclude that the decomposition of 204 calves into clusters C1–C3 is driven by multiple *linked* GSVs (GSVs with correlated *R*-ratios) that represent common genotypes of V genes.

GSVs explain variance in usages of V genes and antibody titers. Clusters C1–C3 are associated with usages of all highly-used V genes except for IGHV1-7 (Figure 4C, Figure S4). Figure 4D shows that the clusters are also associated with antibody titers collected at time point "+6": cluster C1 has higher antibody titers compared to clusters C2 and C3 with P=0.017 according to the Kruskal-Wallis test. This observation suggests that IGenotypes of V genes are associated with the response to the BRD vaccination. Antibody titers collected at three other time points do not have statistically significant associations with clusters C1–C3.

Since the fractions of ultralong antibodies are not associated with clusters C1–C3 (Figure S5), we hypothesize that generation of ultralong antibodies is not specific to genotypes described by the revealed clusters but rather is a general feature of cattle antibody repertoires. However, our analysis revealed subtle correlations between genotypes and some features of ultralong CDR3s. Figure 4E shows that clusters C1–C3 partially explain the variance in Figure 2D: the fraction of ultralong CDR3s among all CDR3s at the time point "+3" positively correlates with titers at the time point "+6" only for animals from the cluster C1 (r=0.32, P=0.0072). Similar correlations do not exist and are not statistically significant for clusters C2 and C3 (r=0.12 and r=0.10, respectively). We thus assume that ultralong CDR3s from the cluster C1 work better in response to the BRD vaccine.

Figure 4F and G show that animals from the cluster C1 are characterized by a lower initial fraction of ultralong CDR3s (in all CDR3s derived from IGHV1-7) and a lower fraction of ultralong CDR3s with six cysteines (important for knob formation) as compared to animals from clusters C2 and C3 (P-values for the cluster variable are 3.96×10^{-4} and 2.63×10^{-5}, respectively). Since the initial number of cysteines in ultralong

335 CDR3s is four (Wang et al., 2013), a higher number of cysteines suggests that ultralong CDR3s of animals
336 from clusters C2 and C3 underwent more extensive affinity maturation before the BRD vaccination
337 compared to animals from the cluster C1. Since the cluster C1 is associated with higher titers after the
338 second BRD vaccination, we extend the hypothesis about pre-existing immunity and suggest that it might
339 partially consist of mature ultralong CDR3s (with six cysteines) generated before the vaccinations in
340 animals from clusters C2 and C3. However, since titers at time points "–3" and "+6" are anticorrelated in
341 all clusters (Figure S6), we also suggest that mature ultralong antibodies might be not the only component
342 of the pre-existing immunity. Further exploration of cattle antibody repertoires would help to understand
343 the origin of the pre-existing immunity (e.g., maternal antibodies or microbiota) and its impact on the BRD
344 vaccination.

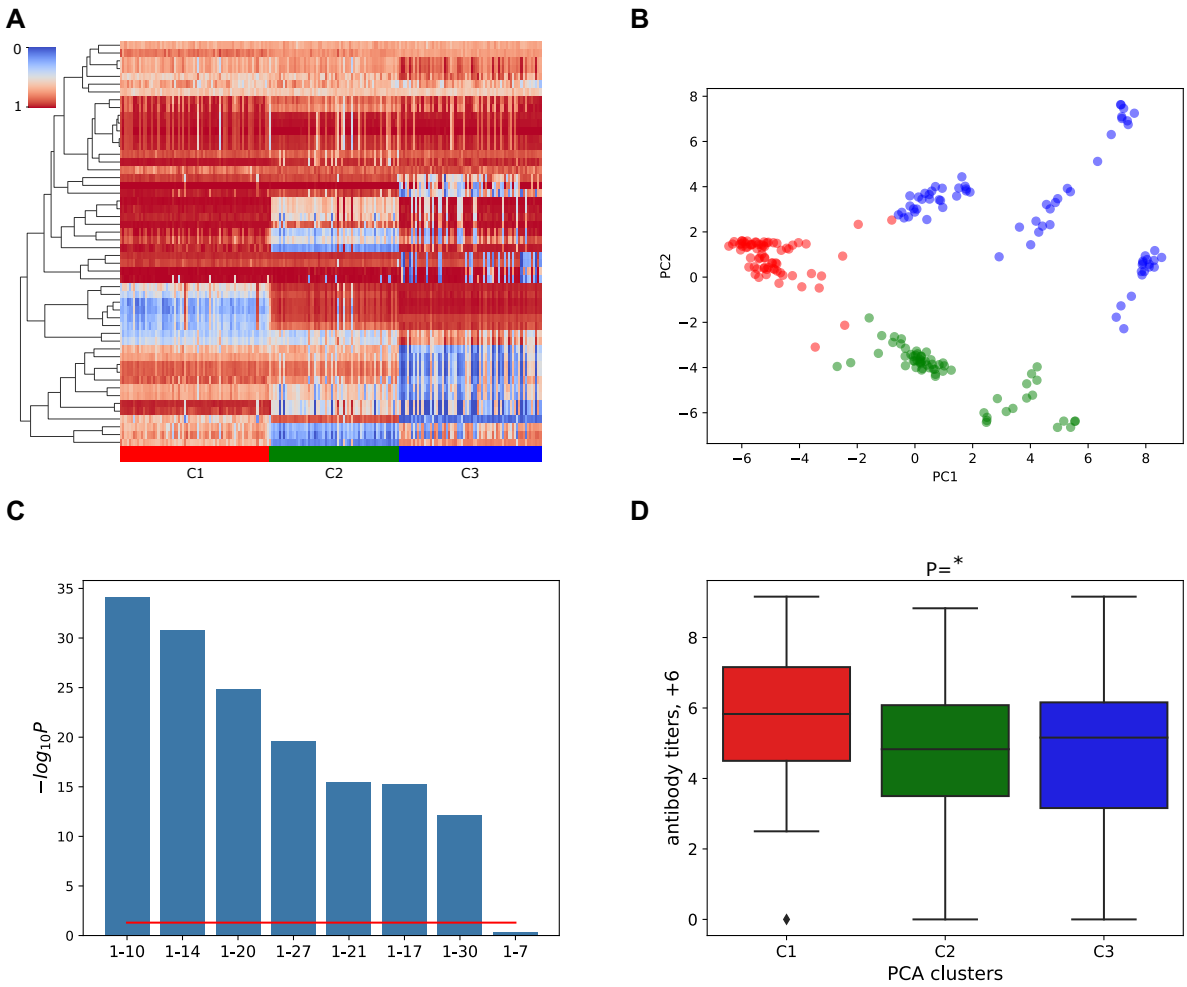

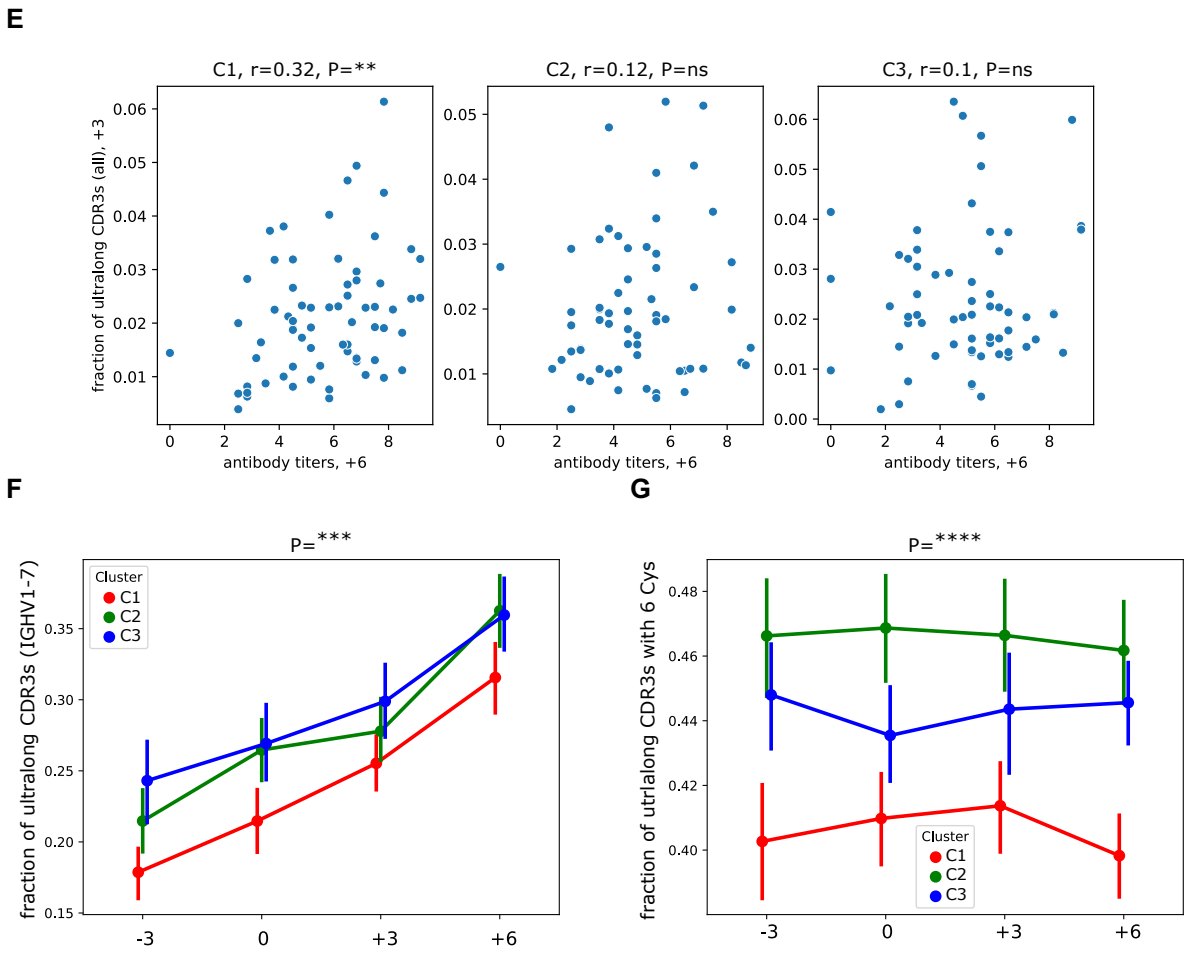

Figure 4. GSVs of V genes are associated with gene usages and antibody titers. (*A*) The 52×204 IGenotype matrix for 52 GSVs of V genes across 204 calves. Rows represent GSVs, columns represent animals. Rows are ordered using the hierarchical clustering, columns are ordered according to the three clusters found using PCA, followed by *k*-means clustering. Three clusters C1, C2, and C3 are shown in red, green, and blue in the lower horizontal panel, respectively. The order of animals within a cluster is chosen arbitrarily. *R*-ratios vary from 0 (blue) to 1 (red). (*B*) Principal components 1 and 2 of the IGenotype matrix shown in (*A*). Three identified clusters are shown in red, green, and blue. (*C*) Likelihoods of association P-values between three PCA clusters and usages of V genes. Usages are computed in the combined datasets. Likelihood is computed as the negative logarithm of the P-value to the base of 10. Genes are shown in the descending order of likelihoods. The red line corresponds to P=0.05. (*D*) Antibody titers at time point "+6" for three PCA clusters. (*E*) Antibody titers at time point "+6" vs fractions of ultralong CDR3s in all CDR3s at time point "+3" across clusters C1–C3. The Pearson correlations (*r*) and P-values (P) are shown at the top of the panel.

(*F*) Fractions of ultralong CDR3s among all CDR3s derived from IGHV1-7 in clusters C1, C2, and C3 at four time points. (*G*) Fractions of ultralong CDR3s with six cysteines among all ultralong CDR3s in clusters C1, C2, and C3 at four time points. Vertical lines in (*F*) and (*G*) show 95% confidence intervals.

A GSV at position 148 in IGHV1-7 is associated with the fraction of ultralong CDR3s. The fraction of ultralong CDR3s among all antibodies varies between 0.0033 and 0.0543 in the combined datasets (Figure S7A). The fraction of ultralong CDR3s limited to CDR3s derived from IGHV1-7 varies from 0.09 to 0.64 in the combined datasets (Figure S7B). Since the clusters C1–C3 are not associated with fractions of ultralong CDR3 antibodies (Figure S5), we also examined potential associations of individual GSVs with fractions of ultralong CDR3s.

The GSV (148, IGHV1-7, A/G) has the most significant association with the fraction of ultralong CDR3s whether computed with all antibodies or limited to IGHV1-7 containing antibodies: $P=3.03\times10^{-28}$ and $P=1.49\times10^{-47}$, respectively (Figure 5A, B). P-values were computed using the linear regression model. The GSV with the next most significant association was GSV (144, IGHV1-17, C/T), but this significance was many orders of magnitude lower (P=0.0016). The closest IGHV1-7 containing GSV in terms of significance was GSV (71, IGHV1-7, C/T) which also has association that is orders of magnitude lower (P=0.0002). Thus, GSV (148, IGHV1-7, A/G) is unique since its association P-values are many orders of magnitude lower than association P-values of all other GSVs.

This GSV (that we refer to as G148A for brevity) also has the most significant association with the usage of IGHV1-7 in the combined dataset ($P=6.11\times10^{-17}$, the linear regression model): the higher is the fraction of nucleotide A at position 148 of IGHV1-7, the higher is the usage of IGHV1-7 (Figure 5C). Figure 5D shows that *R*-ratios of the GSV G148A grow after both vaccinations ($P=3.36\times10^{-204}$). This position was not previously identified as a germline variation (Figure 3B), the known alleles of IGHV1-7 have a nucleotide G at position 148 classified as the second popular nucleotide *N*2 by our analysis (Table S2). The *R*-ratios

of GSV G148A are not associated with clusters C1–C3, suggesting that the GSV is not linked with 47 GSVs which *R*-ratios are associated by clusters C1–C3 (Figure S3). The *R*-ratios for this GSV varies from 0.31 to 0.87, indicating that both nucleotides A and G are always present in Rep-seq reads in each animal (Figure S9A). Figure S9B also shows that *R*-ratios of the GSV grow similarly for clusters C1–C3. We thus assume that GSV G148A is a frequent SHM that is often selected after vaccinations and is important for generating ultralong antibodies.

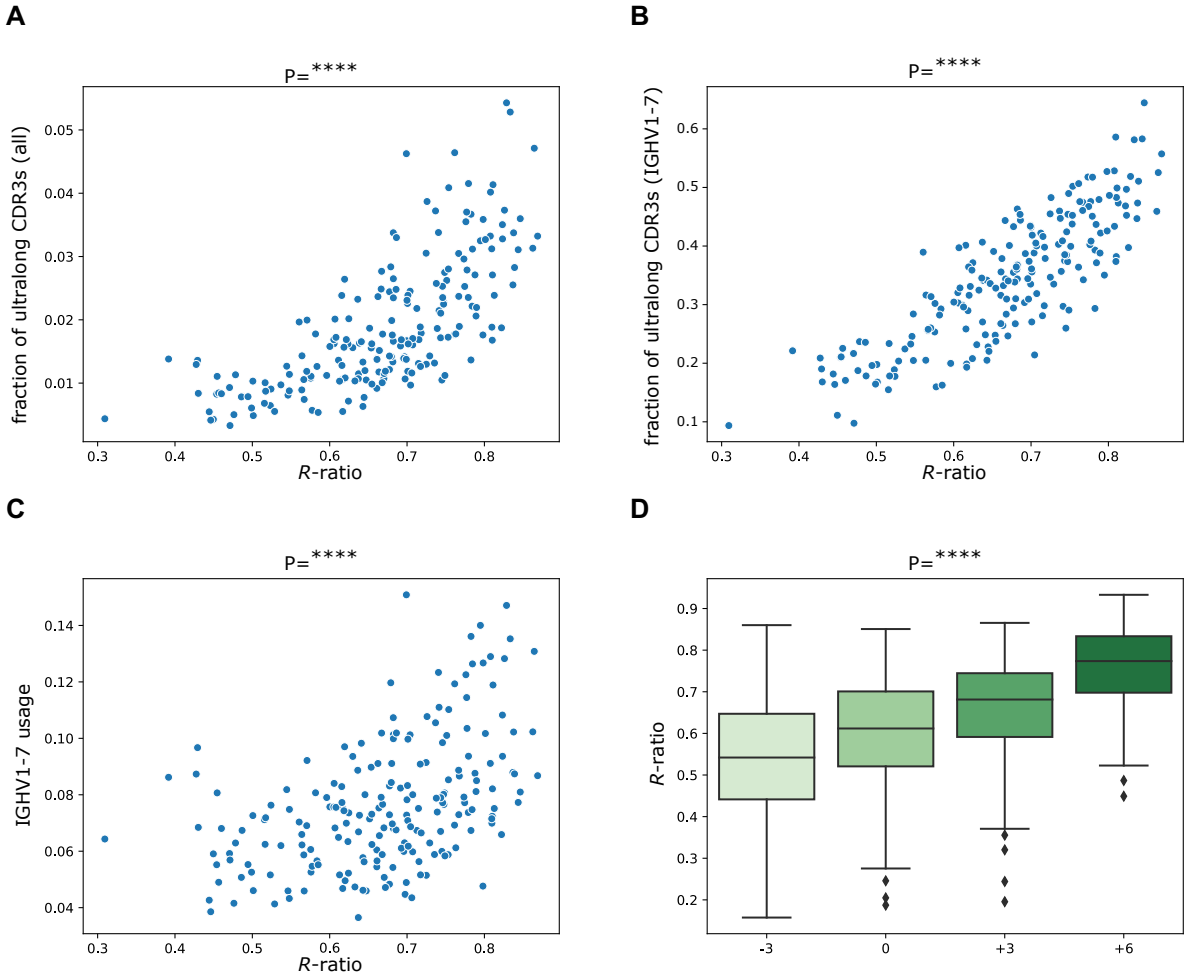

Figure 5. GSV at position 148 of IGHV1-7 is associated with production of ultralong antibodies. (*A*) Fractions of ultralong CDR3s in all CDR3s vs *R*-ratios of the GSV G148A in IGHV1-7. (*B*) Fractions of ultralong CDR3s in all CDR3s derived from IGHV1-7 vs *R*-ratios of the GSV G148A in IGHV1-7. (*C*) Usages of IGHV1-7 in the combined dataset vs *R*-ratios of the GSV G148A at position 148 in IGHV1-7. (*D*) Distributions of *R*-ratios for position 148 in IGHV1-7 at four time points.

392 **The role of the GSV G148A in ultralong CDR3s.** The most abundant nucleotide *N*1=A of the GSV
393 G148A replaces the germline amino acid Gly (encoded by the codon GGT) with the amino acid Ser
394 (encoded by codon AGT) at amino acid position 50. This position represents the last amino acid of the
395 second framework region (FR2) according to the IMGT notation (Lefranc et al., 2003) but is classified as
396 a CDR2 position according to Kabat (Kabat et al, 1979) and Paratome (Kunik et al., 2012) notations. Wang
397 et al., 2013 showed that, unlike Gly at position 50 (referred to as Gly50), Ser at position 50 (referred to as
398 Ser50) can form hydrogen bonds with the conserved Gln at position 97 in the stalk part of an ultralong
399 CDR3. On average, 24.8% and 3.8% of ultralong antibodies derived from IGHV1-7 in the combined
400 datasets contain Ser50 and Gly50, respectively (Figure 6A). In contrast to ultralong antibodies, where Ser50
401 is six-times more frequent than Gly50, Ser50 and Gly50 appear in similar proportions (30.4% and 24.8%,
402 respectively) in non-ultralong CDR3s derived from IGHV1-7 (Figure 6A).
403
404 We also analyzed thirteen 3-D structures of crystallized bovine antibodies (reported by Wang et al., 2013,
405 Stanfield et al., 2016, and Dong et al., 2019) available in the Protein Data Bank (Berman et al., 2000). None
406 of the known ultralong antibodies have the germline Gly at position 50: all but one of them have Ser at
407 position 50 (Figure S10). We further applied the I-Mutant2.0 tool (Capriotti et al., 2005) to analyze the
408 effect of substitutions at this position on the stability of the analyzed antibodies. I-Mutant2.0 generated
409 prediction for only 10 out of 13 analyzed antibodies (three structures were processed with errors) and it
410 turned out that substitution of Ser by the germline amino acid Gly decreases antibody stability for all ten of
411 them (Figure 6B). We thus assume that amino acid Ser at position 50 is critically important for maintaining
412 the structure of ultralong antibodies.
413
414 **Surprising features of ultralong CDR3s.** All ultralong CDR3s are generated through recombination of a
415 148 nt long D gene IGHD8-2 that encodes four cysteines in its third open reading frame and contains 39
416 codons (in the same frame) differing from the cysteine-encoding codons by a single nucleotide, providing

multiple opportunities for generating novel disulfide bonds in an ultralong antibody by somatic mutations of non-cysteines into cysteine. During VDJ recombination, all short IGHD genes undergo intensive exonuclease removals that contribute to the overall diversity of an antibody repertoire (Murphy et al., 2016). To understand the recombination properties of the long IGHD8-2 gene, we collected 2,855,428 distinct ultralong CDR3s across all individuals, aligned them to the IGHD8-2*01 gene, and identified positions corresponding to substitutions, insertions, and deletions. In surprising contrast to the short D genes, the first six and the last three amino acid positions of IGHD8-2 do not accumulate insertions and deletions (Figure 6C) and only the first and last positions undergo substantial numbers of substitutions (Figure 6D). Therefore, in contrast to the short D genes, IGHD8-2 does not undergo extensive truncations from both sides.

The distribution of observed indels in the IGHD8-2*01 segment shows an uneven distribution throughout the middle portion, between positions 6 and 45 (Figure 6C). Relatively increased numbers of indels can be detected in the region between positions 14–17 and downstream from position 25 to 40, with deletions much more common than insertions in the latter. We note that the positions prone to indels do not include those encoding four germline cysteines (positions 2, 12, 18, and 23). Furthermore, the germline cysteine codons accumulate ~5 times fewer substitutions compared to other positions of IGHD8-2 (Figure 6D). Thus, most ultralong CDR3s preserve germline cysteines of IGHD8-2. The introduction of additional cysteines in the ultralong CDR3 by SHM are most commonly the result of substitutions at position 24 (~4 times more common than the average at other positions; Figure 6E).

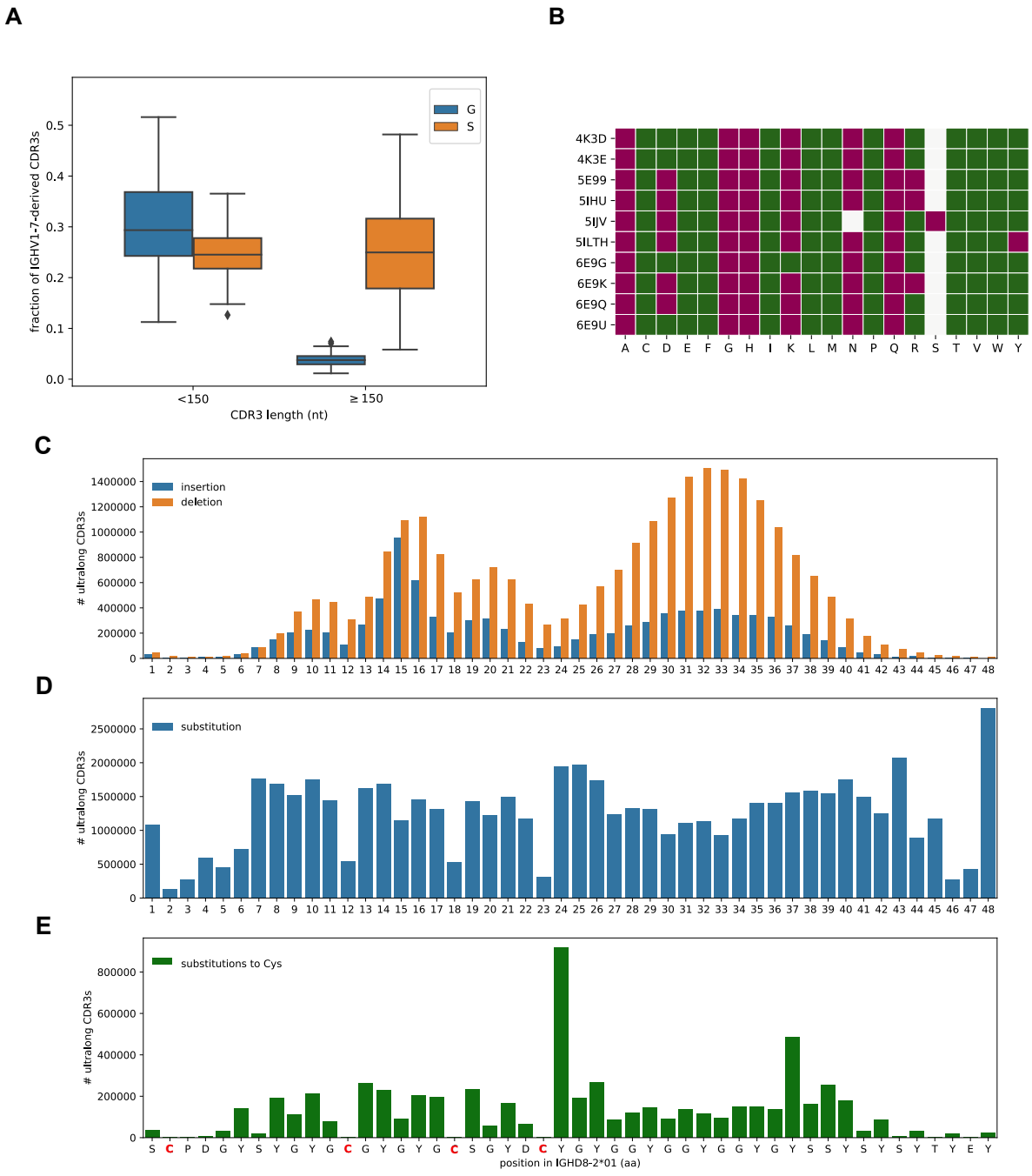

437 **Figure 6. The anatomy of ultralong CDR3s.** (*A*) Fractions of non-ultralong CDR3s (lengths below 150 nt) and
438 ultralong CDR3s derived from IGHV1-7 with amino acids Gly (blue) and Ser (orange) at amino acid position 50.
439 Fractions are computed in the combined datasets. (*B*) Impact of substitutions at position 50 in ten crystallized
440 antibodies predicted by the I-Mutant2.0 tool. Accession IDs of antibody structures are shown on the left. White cells
441 show amino acids at position 50 present in structures (N or S). A green (red) cell (*Ab*, *AA*) indicates that mutation to

442 amino acid *AA* is predicted to increase (decrease) stability of antibody structure *Ab*. (*C–E*) IGHD8-2 is a template for
443 generating cysteines through SHMs. The germline sequence of IGHD8-2*01 is shown at the bottom with four
444 cysteines shown in red. (*C*) The bar plot shows the number of ultralong CDR3s that have insertions (blue) and deletions
445 (orange) at a given position of IGHD8-2*01. The position of insertion is defined as the position in the germline
446 sequence that precedes the insertion. The average lengths of insertions and deletions in IGHD8-2 are 1.6 and 2.4 aa,
447 respectively. (*D*) The bar plot shows the number of ultralong CDR3s that have a substitution at a given position of
448 IGHD8-2*01. (*E*) The bar plot shows the number of ultralong CDR3s that have a substitution into cysteine at a given
449 position of IGHD8-2*01.

450 # Discussion

451 **Longitudinal study of cattle antibody repertoires developed in response to the BRD vaccine.** We
452 conducted a personalized immunogenomics study of 204 calves to analyze the efficacy of the BRD vaccine.
453 Our analysis showed that the BRD vaccinations increase both the usage of IGHV1-7 and the fraction of
454 ultralong antibodies, suggesting that ultralong antibodies play an important role in immune responses
455 against antigens of the BRD vaccine. It also showed that antibody titers measured after the booster
456 vaccination are weakly correlated with the usage of IGHV1-7 and the fraction of ultralong antibodies.
457 Usages of other cattle IGHV genes are not associated with antibody titers before and after the BRD
458 vaccination. We also showed that antibody titers before the initial vaccination anticorrelate with titers after
459 the booster vaccination. This suggests that pre-existing immunity to BRD may prevent successful
460 development of the immune response to the BRD vaccine.
461
462 **The IgQTL analysis of antibody repertoires.** Although the analysis of eQTLs in genomic studies is well
463 developed, there are still no tools for analyzing IgQTLs in immunogenomics datasets. We developed an
464 IgQTL tool for detecting important germline and somatic variations or GSVs (based on analyzing Rep-seq
465 data), applied it to identify GSVs in cattle IGHV genes, and found their associations with various

466 phenotypes (gene usages, fractions of ultralong antibodies, and antibody titers). Our analysis demonstrates
467 that IgQTL can be used for analyzing antigen-specific antibody responses in a population. Although it has
468 only been tested on cattle Rep-seq datasets, it can be applied to any vertebrate species, including humans,
469 and thus improve our understanding of the specifics of adaptive immune responses associated with various
470 antigens.
471
472 **SHM G148A in IGHV1-7 is important for generating ultralong antibodies.** Analysis of the identified
473 GSVs revealed that a GSV G148A in IGHV1-7 is strongly associated with both the usage of IGHV1-7 and
474 the fraction of ultralong antibodies. This GSV results in a substitution of the germline amino acid Gly into
475 Ser that is specific to ultralong antibodies. While non-ultralong antibodies derived from IGHV1-7 have
476 similar fractions of Gly and Ser, the ultralong antibodies have a highly elevated fraction of Ser as compared
477 to the fraction of Gly. Wang et al., 2013 showed that Ser encoded by this GSV forms a hydrogen bond with
478 the conservative Gln at position 95 in the stalk region of an ultralong CDR3. We thus assume that the GSV
479 G148A is not specific to responses induced by the BRD vaccine but rather is a general feature of ultralong
480 antibodies. Different patterns of the GSV G148A in IGHV1-7 in ultralong and non-ultralong antibodies
481 suggest that it represents a frequent SHM rather than a novel germline variation. Further investigation of
482 the origin and the role of this GSV will likely require paired WGS and Rep-seq datasets, as well as analyzing
483 the 3-D structures of ultralong antibodies.
484
485 **Germline variations and SHMs explain variance in titers.** Further analysis of GSVs revealed three
486 clusters (C1, C2, and C3) representing common genotypes of IGHV genes. The detected clusters are
487 associated with usages of all highly-used IGHV genes except for IGHV1-7. The cluster C1 is associated
488 with higher titers after the booster vaccination and a higher correlation between the final titers and the
489 fraction ultralong CDR3s compared to clusters C2 and C3. The cluster C1 is also characterized by a
490 significantly lower fraction of ultralong CDR3s before the vaccination and a lower fraction of ultralong

CDR3s with six cysteines. Since the initial number of cysteines in ultralong CDR3s is four (Wang et al., 2013), a higher number of cysteines indicates that ultralong CDR3s of animals from clusters C2 and C3 underwent more extensive affinity maturation compared to animals from the cluster C1. We conjectured that the pre-existing immunity partially consists of "mature" ultralong CDR3s (with six cysteines) detected before the vaccinations in animals from clusters C2 and C3. However, further exploration of cattle antibody repertoires is needed for understanding the origin of the pre-existing immunity and its impact on the BRD vaccination.

Further analysis of antibody responses to BRD. The GSVs detected by IgQTL might be useful for identifying "vaccine-ready" animals (e.g., animals from the cluster C1) capable of mounting efficient responses to the BRD vaccine. Further studies examining GSVs and their relationship with developing antibody repertoires in response to vaccination have a potential to identify animals with successful responses to the BRD vaccine and thus contribute to the ongoing selection strategies by including not only genomic but also immunogenomic traits.

Our study has revealed that ultralong antibodies play an important role in the antibody response against BRD antigens. Although our study has already combined experimental (Rep-Seq) and computational approaches, these approaches would further benefit from functional experiments aimed at identification of ultralong antibodies that bind BRD antigens. Such experiments (and further antibody engineering analysis) represent the topic of a follow-up paper.

Methods

Sample preparation. The Iowa State University Animal Care and Use Committee (IACUC) approved all animal work before the study was conducted. Purebred American Angus calves (n = 204) were vaccinated with a modified live vaccine (Bovi-Shield Gold 5; Zoetis Inc., Parsippany N.J.) containing antigens of 4

515 viruses associated with bovine respiratory disease as described (Kramer et al., 2017). A second booster
516 vaccination was applied three weeks later. Bovine whole blood was collected and stored in Tempus TM
517 blood RNA tubes (Applied Biosystems, Foster City, CA). Collections occurred at four-time points; three
518 weeks prior to vaccination, at vaccination, three weeks post-vaccination (at booster vaccination), and 3
519 weeks after booster vaccination. RNA was isolated using the Tempus TM spin RNA isolation kit as
520 recommended by the manufacturer (Applied Biosystems, Foster City, CA). Antibody titers were quantified
521 as previously describe (Kramer et al., 2017).
522
523 **Repertoire sequencing.** The RNA was converted to cDNA with the Clontech SMARTer kit (Takara Bio
524 USA; Mountain View, CA) using the modified (Switching Mechanism At 5' End of RNA Transcript) PCR
525 cDNA synthesis protocol (Clontech) and oligonucleotides as described below (Table S3). 2 µg of RNA in
526 11 µl was mixed with 1 µl of 12 µM SMARTer IIA Oligonucleotide. The mixture was incubated at 72 °C
527 for 30 min and then 42 °C for 2 min. 9 µl of master mix, containing 87747 primer, 5X first-strand buffer,
528 0.1M DTT, 10 mM dNTP mix, Recombinant RNasin Ribonuclease inhibitor (Promega), and SuperScript
529 II reverse transcriptase (Invitrogen) was added to the mixture and incubated at 42 °C for 90 min and then
530 70 °C for 10 min. Since primer 87747 (3' SMARTer CDS IIA) targeted on the 5'end of V H leader
531 sequence, the cDNA synthesis produced high quality double strand IgG heavy chain cDNA.
532
533 Illumina amplicon libraries were designed to cover the IgG heavy chain variable region (FR1-4 and CDR1-
534 3) as previously described (Larsen and Smith, 2012). Libraries were constructed by employing two primers
535 that targeted 3' end of the leader region (87934 primer) and 5' end of the IgG heavy chain constant (CH1)
536 region (87935 primer). Table S3 presents information about the primers that were used for this study. For
537 PCR amplification for libraries, AccuPrime Tag DNA polymerase High Fidelity (Invitrogen) with initial
538 denaturation at 94 °C for 2 min, 33 cycles of 94 °C for 15 sec, 64 °C for 15 sec, 68 °C for 1 min, and final
539 extension 68 °C for 5 min conditions were used. The libraries were purified by using AMPure XP bead-

based purification as recommended by the manufacturer (Beckman Coulter, Brea CA). The concentration of libraries was determined by quantitative PCR using a NEBNext library Quant kit for Illumina (New England BioLabs, Ipswich MA). The size of libraries and amplicon profiles were determined by the Fragment Analyzer System (Agilent Technologies, Santa Clara CA). Paired end (2X300 cycle) sequencing was performed on a Miseq® sequencer using a 600 cycle v3 Reagent Kit (Illumina Inc., San Diego CA) producing 300 base paired end reads.

Preprocessing Rep-seq data. Each paired-end read was merged into a single sequence using the PairedReadMerger tool (Safonova et al., 2015). For each resulting sequence, the V gene, the J gene, and the CDR3, contributing to this sequence were inferred using the DiversityAnalyzer tool (Shlemov et al., 2017) based on the cattle germline immunoglobulin genes listed in the IMGT database (Lefranc et al., 2009). To simplify the downstream analysis of gene variations, we kept only the first allele of each V gene and ignored its allele variants. The germline and somatic variations were computed using alignments against the closest V genes reported by the DiversityAnalyzer.

Statistical analysis. Statistical analysis was performed using Python (version 3.8.5). The Kruskal-Wallis test and the Pearson correlation were computed using the Scipy package (version 1.6.0). The linear regression model and the linear mixed effect model were called from the Statmodels package (version 0.12.2).

Data Access. Sequencing datasets were deposited to NCBI BioProject under accession number PRJNA607961 (reviewer's link). Scripts and results are available at GitHub: github.com/yana-safonova/IgQTL.

564 **Competing Interest Statement.** The authors declare that the research was conducted in the absence of any
565 commercial or financial relationships that could be construed as a potential conflict of interest.
566
567 **Acknowledgements.** We are grateful to Vaughn Smider for fruitful discussions and thoughtful comments.
568 We also thank Kristen Kuhn, Jacky Carnahan, and William Thompson for technical support. Mention of
569 trade names or commercial products in this publication is solely for the purpose of providing specific
570 information and does not imply recommendation or endorsement by the U.S. Department of Agriculture.
571 USDA is an equal opportunity provider and employer.
572
573 **Funding:** YS is supported by the UCSD Data Science Fellowship 2017 and the AAI Intersect Fellowship
574 2019. SBS and TLPS are supported by NIFA Award No-2017-67011-26043 and USDA CRIS 3040-31000-
575 100-00-D. CTW is supported in part by NIH, NIAID award No: R21AI142590. PAP is supported by the
576 NIH 2-P41-GM103484PP grant.

577 # References

578 Avnir Y, Watson CT, Glanville J, Peterson EC, Tallarico AS, Bennett AS, Qin K, Fu Y, Huang CY, Beigel JH, Breden
579 F. 2016. IGHV1-69 polymorphism modulates anti-influenza antibody repertoires, correlates with IGHV utilization
580 shifts and varies by ethnicity. *Sci Rep* **6(1):** 1–3.

581 Berman HM, Westbrook J, Feng Z, Gilliland G, Bhat TN, Weissig H, Shindyalov IN, Bourne PE. 2000. The protein
582 data bank. *Nucleic Acids Res* **28(1):** 235–42.

583 Bhalala OG, Nath AP, Inouye M, Sibley CR, UK Brain Expression Consortium. 2018. Identification of expression
584 quantitative trait loci associated with schizophrenia and affective disorders in normal brain tissue. *PLoS Genet* **14(8):**
585 e1007607.

586 Bhardwaj V, Franceschetti M, Rao R, Pevzner PA, Safonova Y. 2020. Automated analysis of immunosequencing
587 datasets reveals novel immunoglobulin D genes across diverse species. *PLoS Comp Bio* **16(4):** e1007837.

588 Burke MJ, Stockley PG, Boyes J. 2020. Broadly Neutralizing Bovine Antibodies: Highly Effective New Tools against
589 Evasive Pathogens? *Viruses* **12(4):** 473.

590 Capriotti E, Fariselli P, Casadio R. 2005. I-Mutant2. 0: predicting stability changes upon mutation from the protein
591 sequence or structure. *Nucleic Acids Res* **33(suppl_2):** W306-10.

592 Corcoran MM, Phad GE, Vázquez Bernat N, Stahl-Hennig C, Sumida N, Persson MA, Martin M, Karlsson Hedestam
593 GB. 2016. Production of individualized V gene databases reveals high levels of immunoglobulin genetic diversity.
594 *Nat Commun* **7:** 13642.

595 Deiss TC, Vadnais M, Wang F, Chen PL, Torkamani A, Mwangi W, Lefranc M-P, Criscitiello MF, Smider VV. 2017.
596 Immunogenetic factors driving formation of ultralong VH CDR3 in Bos taurus antibodies. *Cell Mol Immunol* **14:** 1–
597 12.

598 Dong J, Finn JA, Larsen P, Smith TP, Crowe JE. 2019. Structural Diversity of Ultralong CDRH3s in Seven Bovine
599 Antibody Heavy Chains. *Front Immunol* **10:** 558.

600 Downey, E.D., Tait, Jr., R.G., Mayes, M.S., Park, C.A., Ridpath, G.G., Garrick, D.J., Reecy, M. 2013. An evaluation
601 of circulating bovine viral diarrhea virus type 2 maternal antibody level and response to vaccination in Angus calves.
602 *J Anim Sci* **91(9):** 4440–50.

603 Dudley DD, Chaudhuri, Bassing CH, Alt FW. 2005. Mechanism and control of V(D)J recombination versus class
604 switch recombination: similarities and differences. *Adv Immunol* **86:** 43-112.

605 Economic Research Service, U.S. Department of Agriculture. Cattle & Beef: Sector at a Glance. May 2021.
606 https://www.ers.usda.gov/topics/animal-products/cattle-beef/sector-at-a-glance/.

607 Feeney AJ, Atkinson MJ, Cowan MJ, Escuro G, Lugo G. 1996. A defective Vkappa A2 allele in Navajos which may
608 play a role in increased susceptibility to haemophilus influenzae type b disease. *J Clin Invest* **97(10):** 2277–82.

609 Franco, L.M., Bucasas, K., Wells, J.M., Niño, D. Wang, X., Zapata, G.E., Arden, N., Renwick, A., Yu, P., Quarles,
610 J.M., Bray, M.S., Couch, R.B., Belmont, J.W., Shaw, C.A. 2013. Integrative genomic analysis of the human immune
611 response to influenza vaccination, *eLife* **2:** e00299.

612 Gadala-Maria D, Yaari G, Uduman M, Kleinstein SH. 2015. Automated analysis of high-throughput B-cell sequencing
613 data reveals a high frequency of novel immunoglobulin V gene segment alleles. *Proc Natl Acad Sci USA* **112(8):**
614 E862–70.

615 Gadala-Maria D, Gidoni M, Marquez S, Vander Heiden JA, Kos JT, Watson CT, O'Connor KC, Yaari G, Kleinstein
616 SH. 2019. Identification of Subject-Specific Immunoglobulin Alleles From Expressed Repertoire Sequencing Data.
617 *Front Immunol* **10:** 129.

618 Haakenson JK, Huang R, Smider VV. 2018. Diversity in the cow ultralong CDR H3 antibody repertoire. *Front*
619 *Immunol* **9:** 1262.

620 Heiman GW. 2001. Understanding research methods and statistics: An integrated introduction for psychology.
621 Houghton, Mifflin and Company.

622 Iwasaki A and Yang Y. 2020. The potential danger of suboptimal antibody responses in COVID-19. *Nat Rev Immunol*
623 **20(6):** 339-41.

624 Kabat EA, Te Wu T, Bilofsky H. 1979. Sequences of Immunoglobulin Chains: Tabulation Analysis of Amino Acid
625 Sequences of Precursors, V-regions, C-regions, J-Chain BP-Microglobulins. National Institute of Health.

626 Kramer LM, Mayes MS, Fritz-Waters E, et al. 2017. Evaluation of responses to vaccination of Angus cattle for four
627 viruses that contribute to bovine respiratory disease complex. *J Anim Sci* **95(11):** 4820–34.

628 Kruskal WH and Wallis WW. 1952. Use of Ranks in One-Criterion Variance Analysis. *JASA* **47:** 583-621.

629 Kunik V, Ashkenazi S, Ofran Y. 2012. Paratome: an online tool for systematic identification of antigen-binding
630 regions in antibodies based on sequence or structure. *Nucleic Acids Res* **40(W1):** W521-4.

631 Larsen PA and Smith TP. 2012. Application of circular consensus sequencing and network analysis to characterize
632 the bovine IgG repertoire. *BMC Immunol* **13(1):** 52.

633 Lee JH, Toy L, Kos JT, Safonova Y, Schief WR, Havenar-Daughton C, Watson CT, Crotty S. 2021. Vaccine genetics
634 of IGHV1-2 VRC01-class broadly neutralizing antibody precursor naïve human B cells. *Vaccines* (in press)

635 Lefranc MP, Pommié C, Ruiz M, Giudicelli V, Foulquier E, Truong L, Thouvenin-Contet V, Lefranc G. 2003. IMGT
636 unique numbering for immunoglobulin and T cell receptor variable domains and Ig superfamily V-like domains. *Dev*
637 *Comp Immunol* **27(1):** 55–77.

638 Lefranc MP, Giudicelli V, Ginestoux C, Jabado-Michaloud J, Folch G, Bellahcene F, Wu Y, Gemrot E, Brochet X,
639 Lane J, Regnier L. 2009. IMGT, the international ImMunoGeneTics information system. *Nucleic Acids Res*
640 **37(Database issue):** D1006-12.

641 Lingwood D, McTamney PM, Yassine HM, Whittle JR, Guo X, Boyington JC, Wei CJ, Nabel GJ. 2012. Structural
642 and genetic basis for development of broadly neutralizing influenza antibodies. *Nature* **489(7417):** 566–70.

643 Ma L, Qin T, Chu D, Cheng X, Wang J, Wang X, Wang P, Han H, Ren L, Aitken R, Hammarström L. 2016. Internal
644 Duplications of DH, JH, and C Region Genes Create an Unusual IgH Gene Locus in Cattle. *J Immunol* **196(10):** 4358–
645 66.

646 McDonald JH. 2009. Handbook of biological statistics. Baltimore, MD: Sparky House Publishing.

647 Mikocziova I, Greiff V, Sollid LM. 2021. Immunoglobulin germline gene variation and its impact on human disease.
648 *Genes Immun* **26:** 1–3.

649 Murphy, K., Travers, P., Walport, M., Janeway, C. 2016. Immunobiology. 9th edition. New York: Garland Science.

650 Muyldermans S and Smider VV. 2016. Distinct antibody species: structural differences creating therapeutic
651 opportunities. *Curr Opin Immunol* **40:** 7–13.

652 Parks T, Mirabel MM, Kado J, Auckland K, Nowak J, Rautanen A, Mentzer AJ, Marijon E, Jouven X, Perman ML,
653 Cua T, Kauwe JK, Allen JB, Taylor H, Robson KJ, Deane CM, Steer AC, Hill AVS. 2017. Pacific Islands Rheumatic
654 Heart Disease Genetics Network. Association between a common immunoglobulin heavy chain allele and rheumatic
655 heart disease risk in Oceania. *Nature Commun* **8:** 14946.

656 Safonova Y, Bonissone S, Kurpilyansky E, Starostina E, Lapidus A, Stinson J, DePalatis L, Sandoval W, Lill J,
657 Pevzner PA. 2015. IgRepertoireConstructor: a novel algorithm for antibody repertoire construction and
658 immunoproteogenomics analysis. *Bioinformatics* **31(12):** i53–61.

659 Safonova Y and Pevzner PA. 2019. De novo inference of diversity genes and analysis of non-canonical V (DD) J
660 recombination in immunoglobulins. *Front Immunol* **10:** 987.

661 Shlemov A, Bankevich S, Bzikadze A, Turchaninova MA, Safonova Y, Pevzner PA. 2017. Reconstructing Antibody
662 Repertoires from Error-Prone Immunosequencing Reads. *J Immunol* **199(9):** 3369-80.

663 Sok D, Le KM, Vadnais M, Saye-Francisco KL, Jardine JG, Torres JL, Berndsen ZT, Kong L, Stanfield R, Ruiz J,
664 Ramos A, Liang CH, Chen PL, Criscitiello MF, Mwangi W, Wilson IA, Ward AB, Smider VV, Burton DR. 2017.
665 Rapid elicitation of broadly neutralizing antibodies to HIV by immunization in cows. *Nature* **548(7665):** 108-11.

666 Stanfield RL, Wilson IA, Smider VV. 2016. Conservation and diversity in the ultralong third heavy-chain
667 complementarity-determining region of bovine antibodies. *Sci Immunol* **1(1)**.

668 Taylor JD, Fulton RW, Lehenbauer TW, Step DL, Confer AW. 2010. The epidemiology of bovine respiratory disease:
669 what is the evidence for preventive measures? *Can Vet J* **51(12):** 1351.

670 Thomson CA, Bryson S, McLean GR, Creagh AL, Pai EF, Schrader JW. 2008. Germline V-genes sculpt the binding
671 site of a family of antibodies neutralizing human cytomegalovirus. *EMBO J* **27(19):** 2592-602.

672 Thorndike RL. 1953. Who belongs in the family? *Psychometrika* **18(4):** 267-76.

673 Tonegawa S. 1983. Somatic generation of antibody diversity. *Nature* **302:** 575-81.

674 Walther S, Czerny C-P, Diesterbeck US. 2013. Exceptionally long CDR3H are not isotype restricted in bovine
675 immunoglobulins. *PLoS One* **8(5):** e64234.

676 Wang F, Ekiert DC, Ahmad I, Yu W, Zhang Y, Bazirgan O, Torkamani A, Raudsepp T, Mwangi W, Criscitiello MF,
677 Wilson IA. 2013. Reshaping antibody diversity. *Cell* **153(6):** 1379-93.

678 Watson CT, Glanville J, Marasco WA. 2017. The individual and population genetics of antibody immunity. *Trends*
679 *Immunol* **38(7):** 459-70.

680 Yu L, Guan Y. 2014. Immunologic basis for long HCDR3s in broadly neutralizing antibodies against HIV-1. *Front*
681 *Immunol* **5:** 250.

682 Zimmermann P, Curtis N. 2019. Factors that influence the immune response to vaccination. *Clin Microbiol Rev* **32(2)**.